Supplemental Materials

METHODS

Mice. Male ApoE$^{-/-}$ mice (B6.129P2-ApoE^{tm1Unc}/J) were purchased from The Jackson Laboratory (Bar Harbor) and were fed *ad libitum* with standard chow diet until surgery at 8 to 9 weeks of age. The ApoE^{tm1Unc} mutation was from a 129P2/OlaHsd-derived E14Tg2a embryonic stem cell line and was backcrossed to the C57BL/6J for 10 generations.

Partial carotid ligation surgery. Partial carotid ligation surgeries were performed as previously described[1, 2]. Mice were anesthetized by intra-peritoneal injection of a mixture of xylazine (10 mg/kg) and ketamine (80 mg/kg). The surgical site was epilated, disinfected with Betadine, and a ventral mid-line incision (4 to 5 mm in length) was made in the neck using micro-scissors. The LCA bifurcation was exposed by blunt dissection and three of four caudal LCA branches (left external carotid, internal carotid, and occipital arteries) were carefully dissected free of surrounding connective tissue and ligated with 6-0 silk sutures, leaving the superior thyroid artery intact. The surgical incision was then closed with Tissue-Mend (Veterinary Product Laboratories), and mice were monitored until recovery in a chamber under a heating lamp. Following partial carotid ligation, ApoE$^{-/-}$ mice were maintained for 4 to 28 days on the Paigen's high-fat diet (HFD; Science Diets) containing 1.25% cholesterol, 15% fat, and 0.5% cholic acid[3]. In some studies, sham-ligated animals were operated on as described above except the ligating sutures were not tightened to impede blood flow.

Cells. For flow cytometry analyses of vascular wall leukocytes, partially-ligated male ApoE$^{-/-}$ mice maintained on HFD were sacrificed by CO_2 inhalation and perfused by

cardiac puncture with saline containing 10 U/ml of heparin at 4 days (n=12), 7 days (n=12), 14 days (n=12), 21 days (n=12) and 28 days (n=15) post-ligation. Additionally, sham-ligated ApoE$^{-/-}$ mice (n=9) were fed HFD and sacrificed at 7 days post-surgery. Following sacrifice, LCA and RCA were dissected free of surrounding connective tissue and perivascular fat with care taken not to disrupt associated adventitial tissues and excised by using micro-scissors to cut ~1mm below the carotid bifurcation and ~1 mm above the aortic arch. Leukocytes were isolated as previously described[4]. Excised arteries were placed in ~2 ml of chilled Hanks balanced salt solution, and then pooled (n=3) in 1.5 ml microcentrifuge tubes in 1 ml of chilled digestion buffer consisting of 450 U/ml collagenase I-S, 125 U/ml collagenase XI, 60 U/ml hyaluronidase (Sigma-Aldritch), and 60 U/ml DNAse I (Applichem) in phosphate buffered saline (PBS) supplemented with calcium and magnesium. Pooled arteries were minced finely for 5-10 min using sharp dissection scissors, transferred to a 12-well flat-bottom tissue culture dish, and digested at 37°C for 1 hour at 5% CO_2, with gentle shaking every 15 min. Single cell suspensions were obtained by shearing the digested arteries with a 21½ gauge needle 8-10 times. Cells were transferred to 5 ml FACS tubes (BD Biosciences), washed once in PBS without calcium and magnesium (10 min, 500 *g*, 4°C) and resuspended in 1 ml PBS for staining.

Flow cytometry. Single cell suspensions from pooled carotid artery samples or peripheral blood were incubated for 30 min on ice with Fixable Live/Dead Yellow stain (Invitrogen) to discriminate dead cells, washed once (10 min, 500 *g*, 4°C) in chilled FACS buffer (PBS supplemented with 0.5% bovine serum albumin), and incubated for 10 min on ice with FC Block (2.4G2, BD Biosciences) to prevent nonspecific binding of FC receptors in tissue. Blocked samples were then incubated (30 min, on ice, in dark) with a cocktail containing CD45-biotin (30-F11), CD8a-V450 (53-6.7), CD11c-V450

(HL3), CD4-FITC (RM4-4), Gr-1-FITC (RB6-8C5), CD49b-PE (DX5), NK1.1-PE (PK136), CD3e-PerCP-Cy5.5 (145-2C11), and CD11b-APC-Cy7 (M1/70) monoclonal antibodies (mAb) from BD Biosciences; CD19-PE-Texas Red (6D5) from Invitrogen; and F4/80-PE-Cy7 (BM8) and MHCII-APC (M5/114.15.2) mAb from eBioscience. After staining, cells were washed in chilled FACS buffer, stained with streptavidin-conjugated Qdot 655 (Invitrogen) for 30 min on ice, washed in chilled FACS buffer, and resuspended in BD Stabilizing Fixative (BD Biosciences). Immunofluorescence was detected using a LSR II flow cytometer (BD Immunocytometry Systems) equipped with a 488 nm blue laser, 633 nm red laser, and 405 nm violet laser and set using custom filter settings as follows. Live/Dead Yellow stain was excited using the 405 nm violet laser and detected using a 560/40 dichroic filter with a 550 nm long-pass filter. Qdot 655 fluorescence was excited using the 405 nm violet laser and detected using a 660/20 dichroic filter with a 640 nm long-pass filter. Lastly, to reduce Qdot 655 spillover, a 712/20 dichroic filter with a 685 nm long-pass filter was used to detect PerCP-Cy5.5 fluorescence. In order to determine absolute cell numbers per sample, 50 µl of AccuCount Ultra Rainbow Fluorescent Particles (Spherotech, Inc.) were added to each sample immediately prior to flow cytometry.

Compensation for flow cytometry analyses. Compensation was performed to account for fluorescence spillover of each fluorochrome into multiple detection channels. Anti-rat/hamster IgG-kappa compensation beads (BD Biosciences) were incubated with individual stains of CD8a-V450, CD4-FITC, CD49b-PE, CD19-PE Texas Red, CD3e-PerCP-Cy5.5, F4/80-PE-Cy7, MHCII-APC, and CD11b-APC-Cy7. Single color controls for CD45-Qdot 655 were performed by incubating compensation beads with anti-CD45-biotinylated Ab, followed by streptavidin-conjugated Qdot 655 (Invitrogen). For Live/Dead Yellow compensation, $5x10^5$ splenocytes were heat-killed by incubation at

50°C for 30 min and pooled with $5x10^5$ fresh splenocytes in 1 ml chilled PBS and stained with 1 µl of Live/Dead Yellow (30 min, on ice). In addition to bead-based compensation, populations of fresh and digested splenocytes were single-stained with each individual marker in the panel in order to properly set fluorochrome channel voltages to accommodate adequate signal-to-noise ratios for all cell markers/cell types typed in the panel, and to validate each antibody/fluorochrome pairing for use with digestion[4]. FlowJo analysis software (ver5.0; Tree Star, Inc.) was used to automatically generate an initial compensation matrix using bead-compensated samples. The initial compensation matrix was then manually readjusted using freshly prepared single-stained splenocytes in order to accommodate optimal discrimination of diverse leukocyte populations bearing different auto-fluorescent properties and avoid unnecessary over-compensation artifacts. Lastly, gating strategies were determined using fluorescence minus one (FMO) techniques in which populations of fresh and digested splenocytes were stained with 13 different FMO panels, each lacking one out of the 13 different panel markers (Supplemental Fig. I). This strategy properly accounts for out-of-channel fluorescence as well as any unavoidable compensation artifacts that may remain when determining positive and negative lineage gates[5-7].

Gating strategy for flow cytometry analyses. Splenocytes, peripheral blood leukocytes, or digested arterial wall cells obtained from $ApoE^{-/-}$ mice were incubated with a cell viability marker, followed by 12 different antibodies against cell surface lineage markers and analyzed by flow cytometry (Fig, 1D). Initially, single cell populations were gated based on forward scatter characteristics using FlowJo analysis software (1). Accucount beads were added immediately prior to flow analysis to allow quantification of cell numbers per sample and separated from cells based on ultra-bright fluorescence (2). Live cells were distinguished from dead or damaged cells using a fixable cell

viability stain (Live/Dead Yellow) to substantially reduce background signal (3). Pan-leukocyte anti-CD45 was used to identify leukocytes and filter out non-leukocytic vascular cells such as endothelial cells and vascular smooth muscle cells (4). $CD45^+$ leukocytes were gated into three fractions using anti-CD3 and anti-CD19 coupled to non-overlapping fluorochromes (PerCP-Cy5.5 and PE-Texas Red) to identify T- and B-lymphocytes, and non-lymphocytes ($CD3e^-CD19^-$), respectively (6). Gated cells of the T-lymphocyte ($CD3e^+$) and non-lymphocyte fractions were both labeled with antibodies coupled to FITC and V450. The $CD3e^+$ fraction was divided into $CD4^+$ or $CD8^+$ T-cells using CD4-FITC and CD8a-V450 (6a). Non-lymphocytes ($CD3e^-CD19^-$) were designated as granulocytes using Gr-1 (anti-Ly-6G/Ly-6C)-FITC and NK cells identified using NK1.1 and anti-CD49b coupled to PE (7). Among the remaining myeloid cells, dendritic cells (DCs) were defined as $MHCII^+CD11c^+$ events using MHCII-APC and CD11c-V450 (8). Monocyte/macrophages were identified using antibodies to the pan-monocyte markers F4/80 coupled to PE-Cy7 and CD11b coupled to APC-Cy7 ($F4/80^{+/-}$ $CD11b^+$) (9). The coupling of multiple antibodies to a single fluorochrome was used only when "stacked" markers could be discriminated by a third, independent marker on a different channel (such as CD3e-PerCP-Cy5.5). Cell counts for each cell type and for Accucount beads were calculated by FlowJo software and absolute cell count per carotid artery was determined using the following equation: ((A/B) x (C/D)) x 40, where A = number of cells recorded for the test sample, B = number of AccuCount beads recorded, C = number of AccuCount beads per 50µl (50,000), and D = volume of test sample in µl. Quantification of excluded $CD45^+$ leukocytes was performed using the alternate gating strategy shown in Supplemental Figure IV.

Immunostaining and TUNEL assays. Mice were euthanized and perfused with saline containing heparin as described above. LCA and RCA were collected *en bloc* along with

the heart, aortic arch, trachea, esophagus, and surrounding fat tissue as previously described[2]. Tissue was embedded in optimal cutting temperature (OCT) compound (Tissue-Tek), frozen on liquid nitrogen and stored at –80°C until used. Frozen sections were made starting from the level of the right subclavian artery bifurcation, 300 μm was trimmed away and three sets of ten consecutive 7 μm thick sections were taken at 300 μm intervals constituting the 'proximal' and 'middle' portions of the artery.

Sections were fixed in chilled 4% paraformaldehyde in PBS or a 1:1 mixture of methanol/acetone for 10 min and then blocked (1 hr, at RT) using 0.1% (w/v) BSA or 10% (v/v) goat or donkey serum in PBS. Staining for vascular wall leukocytes was performed overnight at 4°C in a humidified chamber using the following primary antibodies: biotinylated anti-CD45.2 mAb for total leukocytes (104; eBioscience); biotinylated anti-CD11c for DCs (HL3; BD Biosciences); rat anti-mouse CD3 antibody for total T-cells (KT3; ABD Serotec); rat anti-mouse CD68 for macrophages/foam cells (FA-11; ABD Serotec); rat anti-mouse CD11b for myeloid cells/macrophages (M1/70; Abcam); and polyclonal rabbit anti-mouse αSMA for smooth muscle cells (Thermo Scientific). Isotype controls were performed using biotinylated Armenian Hamster IgG (eBio299Arm; eBioscience), biotinylated rat IgG2a, and purified rat IgG2a and IgG2b istoype control Ab (AbD Serotec). Secondary staining was performed using streptavidin-conjugated rhodamine red X (RRX; Invitrogen), DyLight 549-conjugated donkey anti-rat, DyLight 549-conjugated donkey anti-rabbit, streptavidin-conjugated Dylight 549, or RRX-conjugated goat anti-rat secondary antibodies (Jackson Immunoresearch).

In situ apoptosis was measured in cryosections of LCA and RCA using the TUNEL-TMR *In Situ* Cell Death Detection Kit (Roche Applied Science) according to the manufacturer's protocol. In short, freshly thawed cryosections were fixed in 4%

paraformaldehyde in PBS for 20 min at RT and then washed in PBS for 30 min at RT. After 2 more 5 min washes in PBS, 50 μl of TUNEL reaction mixture (TdT enzyme solution with tetramethylrhodamine-dUTP (TMR) labeling solution) was added to the tissue sections and sections were incubated in the dark in a humidified chamber at 37°C for 60 min. Positive control assays were performed by incubating sections in recombinant DNase I for 10 min at RT prior to incubation with the TUNEL reaction mixture. For negative control assays, only TMR labeling solution (without TdT enzyme) was added during incubation with the TUNEL reaction mixture.

Antibody- and TUNEL-stained sections were mounted with Prolong Gold antifade mounting medium with DAPI (Invitrogen). Immunofluorescence stains were imaged using a Zeiss Axioskop 2 Plus fluorescence microscope (Carl Zeiss, Inc.) mounted with a Zeiss Axiocam camera (Carl Zeiss, Inc.). All images were captured with a 40x objective lens using the AxioVision 4 software (Carl Zeiss, Inc.) and modified post-capture to balance brightness and contrast independently for each channel using the AxioVision 4 software, followed by uniform leveling of signal brightness in each color channel using Adobe Photoshop (Adobe Systems, Inc.).

Quantitative analysis of immunofluorescence staining. Frozen cross-sections of LCA and RCA immunostained for CD45 (leukocytes), aSMA (SMCs), and by TUNEL assay (apoptosis) were counterstained with DAPI to identify nuclei as described above. Total $DAPI^+$ nuclei and $CD45^+$, αSMA^+, or $TUNEL^+$ nuclei per artery were quantified for samples obtained 7 days (n=7, from 28 images per stain), 14 days (n=6, from 24 images per stain), and 21 days (n=7, from 28 images per stain) post-ligation using Image J software (NIH). Stains were quantified for additional sham-ligated animals (n=3, from 12

images). For αSMA-stained samples, only intimal nuclei were counted, while intimal, medial, and adventitial nuclei were counted for CD45 and TUNEL stains. The ratio of positive staining nuclei to total $DAPI^+$ nuclei was calculated for all images.

PCR array assay and analysis. LCA and RCA from partially ligated $ApoE^{-/-}$ mice at 4 (n=4), 7 (n=4) or 14 (n=3) days post-ligation were excised as described above and snap frozen in liquid nitrogen. Frozen carotids were then ground by mortar and pestle in 700 µl of Qiazol Lysis Reagent (Qiagen) and total RNA was extracted using the miRNeasy Mini Kit (Qiagen) according to the manufacturer's protocol. cDNA was synthesized using SuperScript III First-Strand Synthesis SuperMix (Invitrogen) according to the manufacturer's protocol. Expression levels of inflammatory cytokine and chemokine genes and their receptors were measured in cDNAs using RT^2 Profiler PCR arrays (SA Biosciences) for inflammatory cytokines & receptors as per manufacturer's protocols and run on a Step-One Plus real time PCR system (Applied Biosystems). Additional qPCR was performed on the same RNA samples as the PCR arrays for *Ifng*, *Tbx21*, *Gata3*, *Rorc*, and *Foxp3* genes using the following primer pairs: *Ifng* (forward 5'-AAC-AAC-CCA-CAG-GTC-CAG-CGC-3'; reverse 5'-CCA-CCC-CGA-ATC-AGC-AGC-GA-3'), *Tbx21* (forward 5'-ATA-CGA-GTG-TCC-CCT-CGC-CAC-C-3'; reverse 5'-CCG-AGG-TGT-CCC-CAG-CCA-GTA-A-3'), *Gata3* (forward 5'-GTG-CCC-GAG-TAC-AGC-TCT-GGA-CT-3'; reverse 5'-AGA-GTC-CGC-AGG-CAT-TGC-AAA-GG-3'), *Rorc* (forward 5'-CCT-TGG-GTG-GCA-GCT-TGG-CTA-GG-3'; reverse 5'-CTT-TTC-CCA-CTT-CCT-CAG-CGC-CC-3'), and *Foxp3* (forward 5'-CAG-CTG-CCT-ACA-GTG-CCC-CTA-GT-3'; reverse 5'-AGG-TGG-TGG-GAG-GCT-GAT-CAT-GG-3'). PCR array data were processed using Microsoft Excel-based RT^2 Profiler PCR Array Data Analysis templates provided by the manufacturer (SA Biosciences). Because housekeeping gene expression increased with lesion development, total copy number per artery was calculated in LCA and RCA

for each target gene and centered to the geometric mean Ct of RCA for all time points using the following equation: 100 / 2^(sample Ct – mean RCA Ct).

Cytokine bead array (CBA) ELISA assay. LCA and RCA from partially ligated ApoE$^{-/-}$ mice were excised as described above and cultured overnight in 60 µl of DMEM supplemented with 10% fetal calf serum, 100 U/mL penicillin, and 100 µg/mL streptomycin at 37°C in 5% CO_2 as previously described[8]. During this time, vascular cytokine production was stimulated by adding 12-O-tetradecanoylphorbol-13-acetate (TPA, 10 µmol/L) and ionomycin (2 µmol/L; Cell Signaling Technology) to the tissue culture medium. Following incubation, levels of cytokines TNFα, IFNγ, IL-2, IL-4, and IL-5 were measured using the cytokine bead array ELISA kit (BD Biosciences; San Jose, CA) according to manufacturer's protocol. Cytokine levels were detected using a LSR II flow cytometer (BD Immunocytometry Systems). CBA array data were processed using FCAP Array software (Soft Flow, Inc.). The theoretical limit of detection for the cytokines measured was 5.0 pg/ml (IL-2), 5.0 pg/ml (IL-4), 5.0 pg/ml (IL-5), 2.5 pg/ml (IFN-γ), and 6.3 pg/ml (TNFα).

Partial least squares regression (PLSR) modeling analysis. To extract relationships between changes in gene expression and cell infiltration dynamics over the time course of flow-disturbed atherosclerosis, a multivariate analysis method, partial least squares regression (PLSR), was applied to the quantitative flow cytometry and PCR array data collected at days 4, 7, and 14 post-ligation. This technique is useful for extracting relationships across multiple types of quantitative data and multiple treatment conditions and has been successfully used to derive information for signal transduction network features[9], viral infection[10], and cell fate decisions[11-13]. The algorithm finds an optimal set

of “latent variables”, or principal components, that best captures the variance in the data through a linear combination of the X-variables (qPCR raw Ct values), as well as optimizing the regression to a dependent Y-variable set (number of immune cells counted by flow cytometry).

The multivariate analysis was performed as previously described[14]. Briefly, an *m x n* data matrix was created where *m* =97 represents the concatenated columns of each mRNA evaluated by qPCR (X-variables) along with flow cytometry values (Y-variables), and *n* =28 rows represent the “observations”, individual samples collected at each day in LCA or RCA. The matrix was pre-processed by log transformation to achieve normal distributions of observations, then mean-centered and unit-variance scaled to prevent biasing of the variables in the model. Models were generated using SIMCA-P software (Umetrics) and evaluated based upon the variance captured (Q^2 value) and goodness of fit (R^2Y). Genes that were statistically insignificant in a given component were trimmed from the model, which further enhanced the regression fit.

Statistical analysis. Values are expressed as mean±SEM unless otherwise indicated. Pairwise comparisons were performed using one-way or two-way t-tests. Multiple comparisons of means were performed using 1-way ANOVA followed by Tukey’s Multiple Comparison tests. Differences between groups were considered significant at P values below 0.05. All statistical analyses were performed using Prism software (GraphPad Software).

SUPPLEMENTAL DATA

Supplemental Table I. Time course analyses of dynamic leukocyte accumulation in flow-disturbed LCA

Comparison	Mean Diff.	q	Significant? P<0.05?	Summary	ANOVA P value
Leukocytes					0.0002
4v7	86.78	8.56	Yes	***	
7v14	-63.19	6.23	Yes	**	
7v21	-70.19	6.92	Yes	**	
7v28	-63.11	6.56	Yes	**	
B-cells					0.0249
4v7	0.32	1.01	No	ns	
7v14	0.49	1.54	No	ns	
7v21	1.31	4.11	No	ns	
7v28	0.33	1.09	No	ns	
T-cells					0.0350
4v7	2.90	5.11	Yes	*	
7v14	-1.29	2.28	No	ns	
7v21	-1.12	1.98	No	ns	
7v28	-1.60	2.98	No	ns	
Dendritic Cells					0.0012
4v7	20.38	7.30	Yes	***	
7v14	-12.87	4.61	Yes	*	
7v21	-16.13	5.77	Yes	**	

7v28	-14.92	5.63	Yes	**	
NK Cells					0.0040
4v7	5.24	6.13	Yes	**	
7v14	-3.08	3.61	No	ns	
7v21	-3.29	3.86	No	ns	
7v28	-4.75	5.86	Yes	**	
Monocyte/Macrophages					<0.0001
4v7	48.76	9.24	Yes	***	
7v14	-41.82	7.93	Yes	***	
7v21	-44.54	8.44	Yes	***	
7v28	-37.48	7.49	Yes	***	
Granulocytes					0.0298
4v7	2.54	4.11	No	ns	
7v14	-0.58	0.93	No	ns	
7v21	-2.18	3.54	No	ns	
7v28	-0.37	0.63	No	ns	

Supplemental Table II. PCR array of cytokines and chemokines expressed in LCA and RCA, and their known functions.

A. 7 day post-ligation

Gene Symbol	Gene Name	Fold Change (LCA/RCA)	p value	Function
Chemokine Genes				
Ccl2	chemokine (C-C motif) ligand 2	138.19	0.0169	**Attracts:** monocytes, memory T-cells, DCs
Ccl7	chemokine (C-C motif) ligand 7	107.47	0.0476	**Attracts:** monocytes **Activates:** macs
Ccl5	chemokine (C-C motif) ligand 5	38.06	0.0250	**Attracts:** T-cells **Activates:** NK cells
Cxcl12	chemokine (C-X-C motif) ligand 12	34.26	0.0123	**Attracts**: lymphocytes
Ccl12	chemokine (C-C motif) ligand 12	32.06	0.0275	**Attracts:** monocytes, lymphocytes
Ccl6	chemokine (C-C motif) ligand 6	31.55	0.0427	**Expressed by:** neutrophils, macs
Cxcl9	chemokine (C-X-C motif) ligand 9	19.51	0.0310	**Attracts:** T-cells
Ccl22	chemokine (C-C motif) ligand 22	12.07	0.0030	**Expressed by:** macrophages, DCs
Ccl19	chemokine (C-C motif) ligand 19	11.55	0.0481	**Attracts:** B-cells, $CCR7^+$ T-cells, DCs

Ccl9	chemokine (C-C motif) ligand 9	10.71	0.0230	**Attracts:** $CD11b^+$ DCs
Cx3cl1	chemokine (C-X3-C motif) ligand 1	10.26	0.0210	**Attracts:** T-cells, monocytes, DCs
Cxcl10	chemokine (C-X-C motif) ligand 10	10.25	0.0405	**Attracts:** monocytes, T-cells, NK cells, DCs
Ccl4	chemokine (C-C motif) ligand 4	9.78	0.0034	**Attracts:** monocytes, NK cells
Ccl3	chemokine (C-C motif) ligand 3	9.43	0.0002	**Attracts:** neutrophils
Ccl24	chemokine (C-C motif) ligand 24	3.50	0.0242	**Attracts:** eosinophils, resting T-cells, neutrophils
Ccl1	chemokine (C-C motif) ligand 1	2.33	0.0137	**Attracts:** monocytes, NK cells, immature B-cells
Chemokine Receptor Genes				
Ccr5	chemokine (C-C motif) receptor 5	95.85	0.0305	**Binds:** CCL5, CCL3, CCL4
Ccr3	chemokine (C-C motif) receptor 3	93.04	0.0377	**Binds:** CCL11, CCL26, CCL7, CCL13, CCL5
Ccr2	chemokine (C-C motif) receptor 2	57.08	0.0497	**Binds:** CCL2
Cxcr3	chemokine (C-X-C motif) receptor 3	13.35	0.0026	**Binds:** CXCL9, CXCL10, CXCL11,

				CXCL4
Cxcr2	chemokine (C-X-C motif) receptor 2	11.64	0.0286	**Binds:** IL8, CXCL1, CXCL2, CXCL3, CXCL5
Cxcr4	chemokine (C-X-C motif) receptor 4	10.39	0.0258	**Binds:** CXCL12
Ccr9	chemokine (C-C motif) receptor 9	7.27	0.0082	**Binds:** CCL25
Ccr7	chemokine (C-C motif) receptor 7	6.51	0.0243	**Binds:** CCL19
Ccr6	chemokine (C-C motif) receptor 6	6.13	0.0122	**Binds:** CCL20
Cytokine Genes				
Mif	macrophage migration inhibitory factor	30.23	0.0236	Macrophage fx
Tgfb1	transforming growth factor, beta 1	16.39	0.0052	Anti-inflammatory
Il1a	interleukin 1 alpha	13.32	0.0001	Pro-inflammatory
Aimp1	aminoacyl tRNA synthetase complex-interacting multifunctional protein 1	10.91	0.0336	Pro-inflammatory
Il16	interleukin 16	10.03	0.0258	T-cell activation **Attracts:** activated $CD4^+$ T-cells, $CD4^+$ DCs

Il18	interleukin 18	8.81	0.0030	Pro-inflammatory
Il1f6	interleukin 1 family, member 6	4.95	0.0170	?
Il15	interleukin 15	4.86	0.0312	NK cell activation / proliferation; homeostatic T-cell proliferation
Tnf	tumor necrosis factor	4.35	0.0390	Pro-inflammatory
Il4	interleukin 4	4.26	0.0298	Th2 T-cell differentiation
Il1f8	interleukin 1 family, member 8	4.08	0.0271	?
Il11	interleukin 11	3.65	0.0299	Platelet production; lymphopoeisis
Il13	interleukin 13	2.68	0.0425	Allergic inflammation
Cytokine Receptor Genes				
Il2rg	interleukin 2 receptor, gamma chain	104.87	0.0008	Common γ-chain subunit for IL2, IL4, IL7, IL9, IL15, IL21 receptors
Il10ra	interleukin 10 receptor, alpha	72.15	0.0067	Subunit of IL10 receptor
Il13ra1	interleukin 13 receptor, alpha 1	31.21	0.0064	Common subunit for IL13 and IL4 receptors
Il10rb	interleukin 10 receptor, beta	25.30	0.0016	Subunit of IL10

				receptor
Il6st	interleukin 6 signal transducer	19.63	0.0131	
Tnfrsf1a	tumor necrosis factor receptor superfamily, member 1a	14.78	0.0221	TNF receptor
Il2rb	interleukin 2 receptor, beta chain	9.77	0.0033	IL2 receptor subunit
Il6ra	interleukin 6 receptor, alpha	9.72	0.0206	IL6 receptor subunit
Il1r2	interleukin 1 receptor, type II	7.37	0.0312	IL1A / IL1B antagonist
Other Inflammatory Genes				
Spp1	secreted phosphoprotein 1	162.32	0.0048	Th1 differentiation; anti-apoptosis; neutrophil / mast cell migration
Itgb2	integrin beta 2	113.49	0.0001	Leukocyte adhesion / extravasation
Itgam	integrin alpha M	24.34	0.0203	CD11b antigen
Casp1	caspase 1	23.31	0.0002	Cell necrosis; IL-1β and IL-18 synthesis
Abcf1	ATP-binding cassette, sub-family F (GCN20), member 1	6.11	0.0033	?
Bcl6	B-cell leukemia/lymphoma 6	4.85	0.0149	IL-4 synthesis (B-cells)

B. 14 day post-ligation

Gene	Fold	p	Function

Symbol	Gene Name	Change (LCA/RCA)	value	
Chemokine Genes				
Ccl6	chemokine (C-C motif) ligand 6	994.86	0.0480	**Expressed by:** neutrophils, macs
Ccl2	chemokine (C-C motif) ligand 2	716.07	0.0047	**Attracts:** monocytes, memory T-cells, DCs
Ccl9	chemokine (C-C motif) ligand 9	83.36	0.0231	**Attracts:** $CD11b^+$ DCs
Ccl12	chemokine (C-C motif) ligand 12	69.38	0.0346	**Attracts:** monocytes, lymphocytes
Ccl22	chemokine (C-C motif) ligand 22	61.52	0.0004	**Expressed by:** macrophages, DCs
Ccl19	chemokine (C-C motif) ligand 19	60.53	0.0452	**Attracts:** B-cells, $CCR7^+$ T-cells, DCs
Ccl4	chemokine (C-C motif) ligand 4	57.61	0.0084	**Attracts:** monocytes, NK cells
Ccl3	chemokine (C-C motif) ligand 3	56.19	0.0281	**Attracts:** neutrophils
Ccl5	chemokine (C-C motif) ligand 5	53.51	0.0086	**Attracts:** T-cells **Activates:** NK cells
Cx3cl1	chemokine (C-X3-C motif) ligand 1	51.79	0.0004	**Attracts:** T-cells, monocytes, DCs
Cxcl9	chemokine (C-X-C motif) ligand 9	31.22	0.0148	**Attracts:** T-cells

Ccl17	chemokine (C-C motif) ligand 17	19.42	0.0057	**Attracts:** T-cells
Ccl24	chemokine (C-C motif) ligand 24	15.87	0.0049	**Attracts:** eosinophils, resting T-cells, neutrophils
Ccl25	chemokine (C-C motif) ligand 25	7.90	0.0273	**Attracts:** T-cells, macrophages, DCs
Ccl1	chemokine (C-C motif) ligand 1	5.99	0.0030	**Attracts:** NK cells, monocytes, immature B-cells
Ccl20	chemokine (C-C motif) ligand 20	3.55	0.0259	**Attracts:** lymphocytes, neutrohpils, DCs
Chemokine Receptor Genes				
Ccr2	chemokine (C-C motif) receptor 2	165.90	0.0382	**Binds:** CCL2
Ccr1	chemokine (C-C motif) receptor 1	141.64	0.0224	**Binds:** CCL3, CCL5, CCL7, CCL23
Cxcr3	chemokine (C-X-C motif) receptor 3	39.99	0.0371	**Binds:** CXCL9, CXCL10, CXCL11, CXCL4
Ccr6	chemokine (C-C motif) receptor 6	30.28	0.0029	**Binds:** CCL20
Ccr7	chemokine (C-C motif) receptor 7	24.69	0.0053	**Binds:** CCL19

Ccr10	chemokine (C-C motif) receptor 10	12.72	0.0126	**Binds:** CCL27
Cxcr5	chemokine (C-X-C motif) receptor 5	11.48	0.0453	**Binds:** CXCL13
Ccr4	chemokine (C-C motif) receptor 4	7.10	0.0217	**Binds:** CCL2, CCL4, CCL5, CCL17, CCL22
Cytokine Genes				
Tgfb1	transforming growth factor, beta 1	276.70	0.0106	Anti-inflammatory
Il15	interleukin 15	73.47	0.0151	NK cell activation / proliferation; homeostatic
Il1b	interleukin 1 beta	56.06	0.0384	Pro-inflammatory T-cell activation
Il16	interleukin 16	50.28	0.0334	**Attracts:** activated $CD4^+$ T-cells, $CD4^+$ DCs
Aimp1	aminoacyl tRNA synthetase complex-interacting multifunctional protein 1	44.77	0.0267	Pro-inflammatory
Il1f6	interleukin 1 family, member 6	24.51	0.0046	?
Il18	interleukin 18	22.96	0.0247	Pro-inflammatory

Il4	interleukin 4	21.73	0.0103	Th2 T-cell differentiation
Il1f8	interleukin 1 family, member 8	20.08	0.0037	?
Il17b	interleukin 17B	17.83	0.0087	Pro-inflammatory
Ltb	lymphotoxin B	17.58	0.0210	Pro-inflammatory
Il13	interleukin 13	15.74	0.0016	Allergic inflammation
Il11	interleukin 11	6.09	0.0498	Platelet production; lymphopoeisis
Il3	interleukin 3	4.50	0.0401	Myeloid progenitor cell differentiation
Cytokine Receptor Genes				
Il2rg	interleukin 2 receptor, gamma chain	456.61	0.0252	Common γ-chain subunit for IL2, IL4, IL7, IL9, IL15, IL21 receptors
Il13ra1	interleukin 13 receptor, alpha 1	292.70	0.0157	Common subunit for IL13 and IL4 receptors
Il10ra	interleukin 10 receptor, alpha	290.38	0.0150	Subunit of IL10 receptor
Il10rb	interleukin 10 receptor, beta	172.21	0.0093	Subunit of IL10 receptor
Il6st	interleukin 6 signal transducer	111.75	0.0202	

Il1r1	interleukin 1 receptor, type I	98.54	0.0346	
Tnfrsf1a	tumor necrosis factor receptor superfamily, member 1a	87.87	0.0309	TNF receptor
Il2rb	interleukin 2 receptor, beta chain	55.44	0.0049	IL2 receptor subunit
Il6ra	interleukin 6 receptor, alpha	39.71	0.0011	IL6 receptor subunit
Other Inflammatory Genes				
Spp1	secreted phosphoprotein 1	15057.95	0.0258	Th1 differentiation; anti-apoptosis; neutrophil / mast cell migration
Itgb2	integrin beta 2	958.06	0.0288	Leukocyte adhesion / extravasation
Casp1	caspase 1	128.06	0.0185	Cell necrosis; IL-1β and IL-18 synthesis
Abcf1	ATP-binding cassette, sub-family F (GCN20), member 1	28.73	0.0113	?
Bcl6	B-cell leukemia/lymphoma 6	14.13	0.0146	IL-4 synthesis (B-cells)
Tollip	toll interacting protein	11.45	0.0141	Inhibits TLR signaling

Supplemental Figure I.

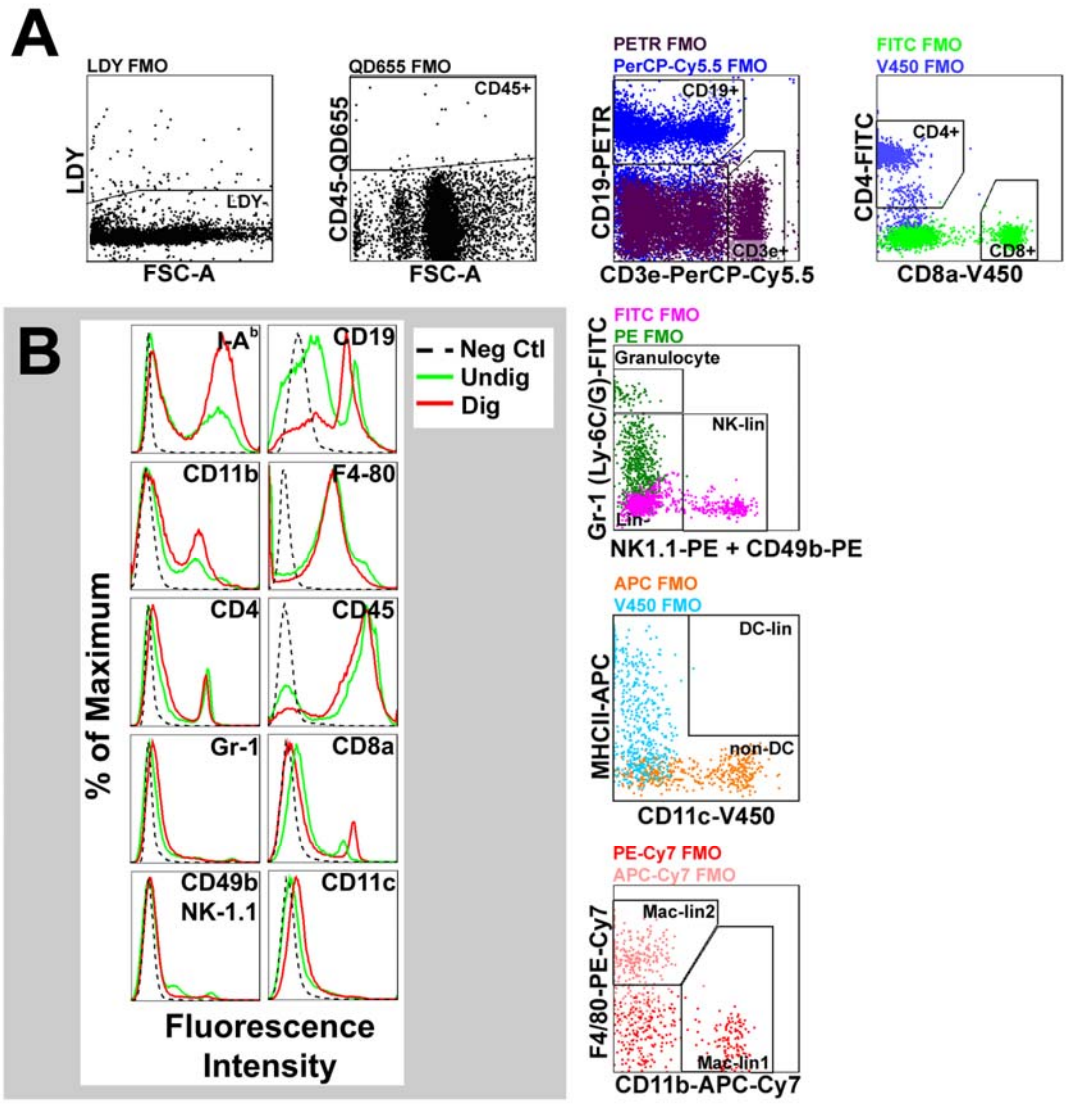

Supplemental Figure I. Fluorescence minus one gating controls and single-color stain controls for 13-parameter flow cytometry method. *A*, Fluorescence minus one (FMO) control staining was performed on digested C57/Bl6 splenocytes in order to determine appropriate gate assignments for the 13-parameter flow cytometry method. Dot plots above show FMO samples and gate assignments for each step of the gating strategy (Fig. 1D). The displayed antibody/fluorochrome conjugates are identified at the left and bottom of each plot. Excluded fluorochromes are listed at the top of each plot. For bivariate plots of multiple fluorochromes, excluded fluorochromes labels are color-coded to match their corresponding dot plots. *B*, Single-color stain controls were performed on enzymatically digested (red histograms) and undigested (green histograms) splenocytes. Dotted black histograms denote unstained negative controls. In (A), FSC-A, forward scatter area; LDY, Live/Dead Yellow stain; QD655, Quantum Dot 655; PETR, PE-Texas Red.

Supplemental Figure II.

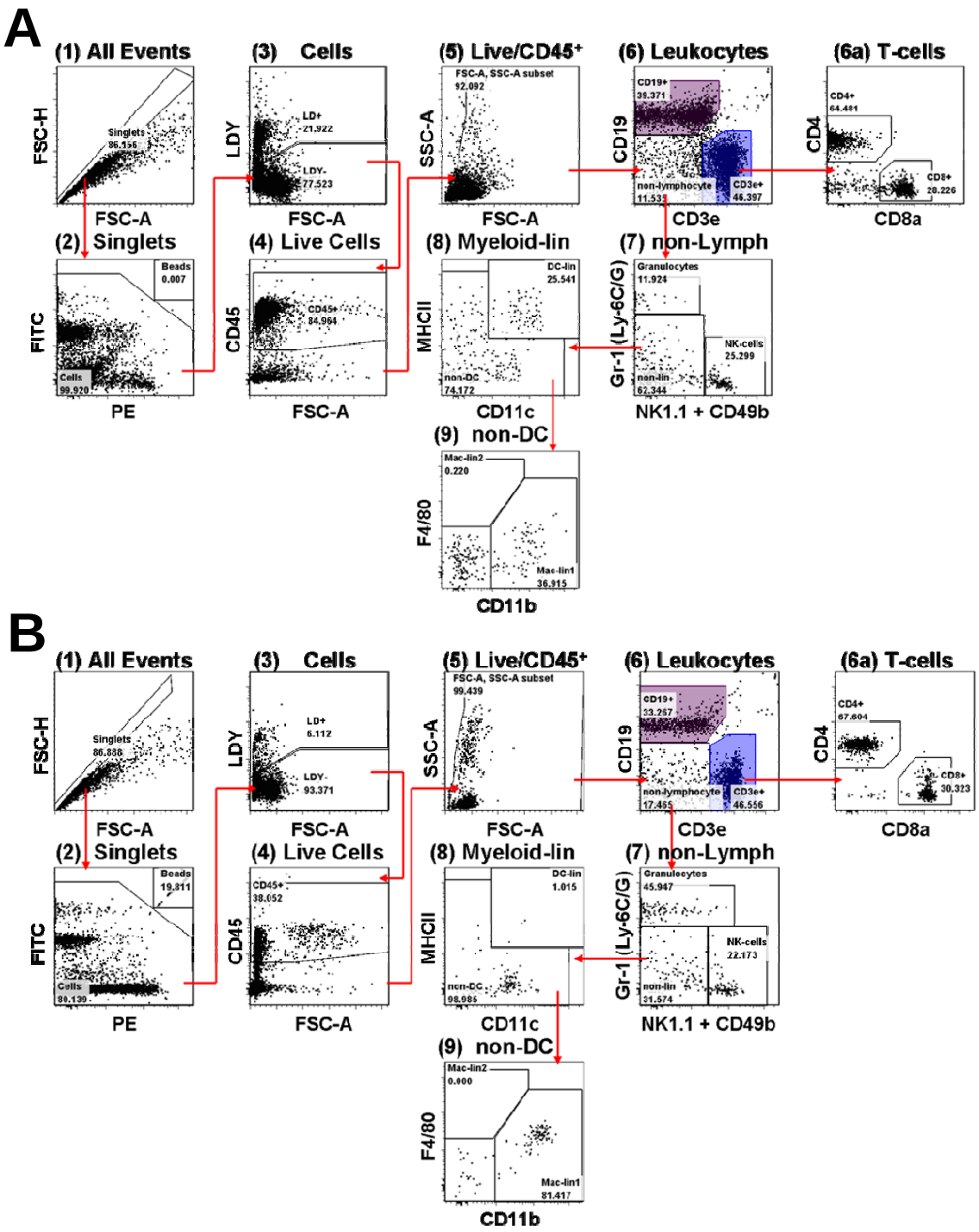

Supplemental Figure II. Thirteen-parameter, 10-channel flow cytometry staining in splenocytes and peripheral blood leukocytes. Splenocytes and peripheral blood leukocytes (PBL) were harvested from untreated 8wk-old male ApoE$^{-/-}$ mice and phenotyped using the 13-paramter flow cytometry method. *A,* Splenocytes were harvested by forcing spleen tissue through a 100 μm filter. Shown is a representative staining of undigested splenocytes. *B,* PBL were drawn by puncture of the descending aorta. Shown is a representative staining. Dot plots show appropriate leukocyte composition for both tissue compartments including increased DC (CD11c^{+}MHCII^{+}) levels in spleen compared with blood, and increased granulocyte (Ly6-C/G^{hi}) levels in the blood. Numbers indicate percent of parent. FSC-H, forward scatter height; FSC-A forward scatter area; SSC-A, side scatter area; LDY, Live/Dead Yellow stain.

Supplemental Figure III.

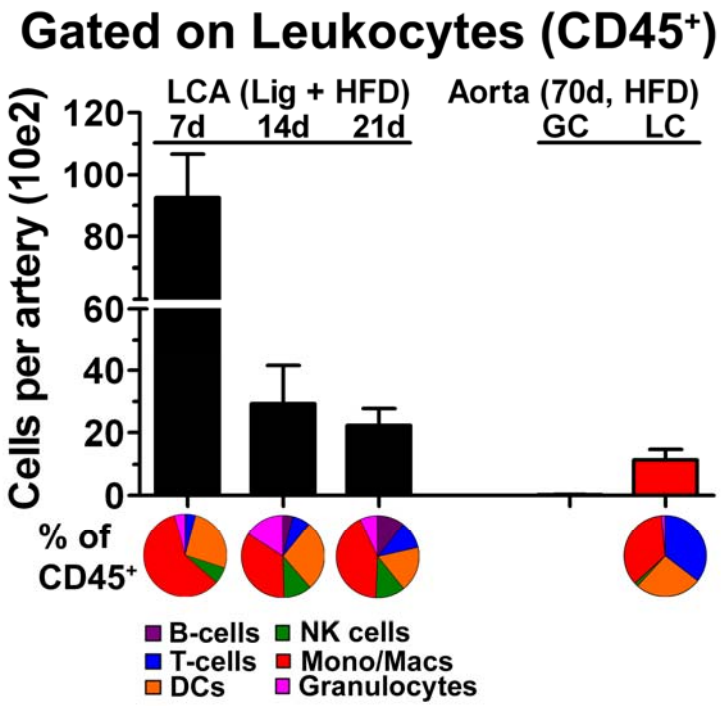

Supplemental Figure III. Comparison of carotid and aortic lesions using the 13-parameter flow cytometry method. Leukocyte preparations from LCA taken 7, 14, 21, and 28 days post-ligation were compared with aortic leukocyte preparations from ApoE$^{-/-}$ mice fed a high-fat diet (HFD) for 70 days (10 weeks), in which athero-resistant aortic greater curvature (GC) and atheroprone lesser curvature (LC) were excised, pooled (n=3), and digested independently. Graph depicts absolute leukocyte numbers per artery. Pie charts below graph depict compositional analyses of total leukocyte data. n=4 for LCA samples; n=2 for aortic samples.

Supplemental Figure IV.

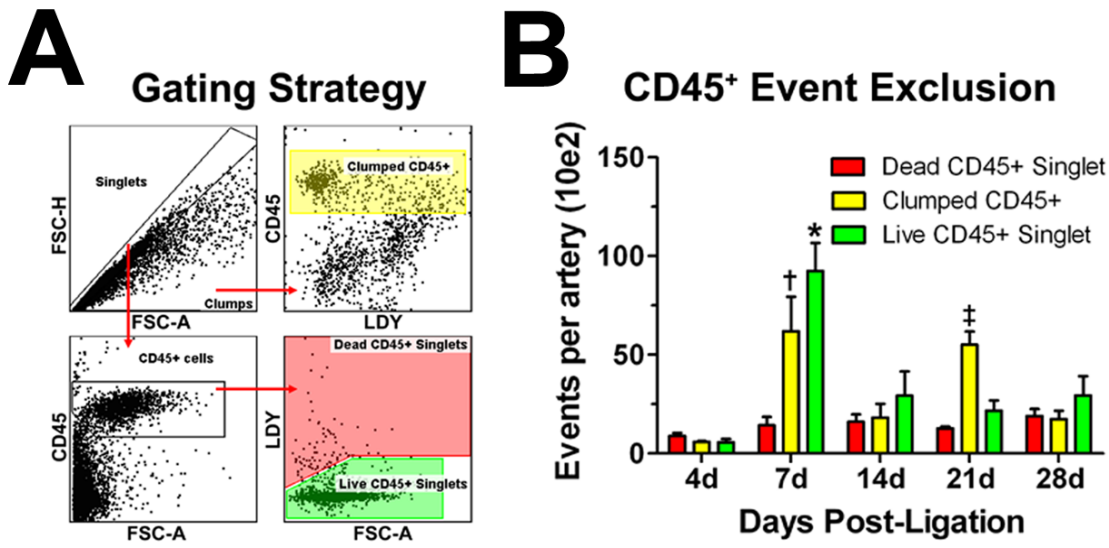

Supplemental Figure IV. Sample quality and leukocyte viability remain fairly consistent between cell preparations from early and developed plaques. *A*, The flow cytometry data from Figure 2A was further analyzed as shown in a representative gating scheme. *B,* The number of non-viable ($CD45^+LDY^+$; red bars) and non-singlet, or "clumped" (yellow bars) vascular leukocytes from LCA were quantified and compared against live $CD45^+$ singlets (green bars). Data are mean values ±SEM. In (B), *, $p<0.05$, 7d versus 4d, 14d, 21d, and 28d; †, $p<0.05$ versus 4d, 14d, and 28d; ‡, $p<0.05$ versus 4d.

Supplemental Figure V.

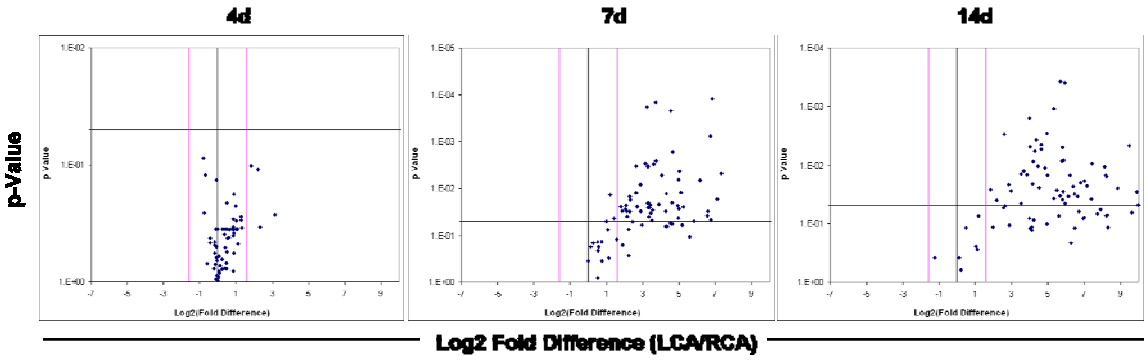

Supplemental Figure V. Cytokine and chemokine gene expression is upregulated by disturbed flow in partially-ligated LCA. Total RNAs obtained from LCA and RCA at 4 (n=4), 7 (n=4), or 14 (n=3) days post-ligation in ApoE$^{-/-}$ mice fed the HFD were analyzed by PCR cytokine arrays (shown in Fig. 5A). Shown are volcano plots depicting significant increases in cytokine and chemokine gene expression in flow-disturbed LCA compared to contralateral RCA. Red lines denote significant thresholds for magnitude of fold changes ($-3 \geq x \geq 3$); blue lines denote significance threshold ($p < 0.05$) for Student t-tests; each blue dot represents mean fold change in the expression of one gene.

Supplemental Figure VI.

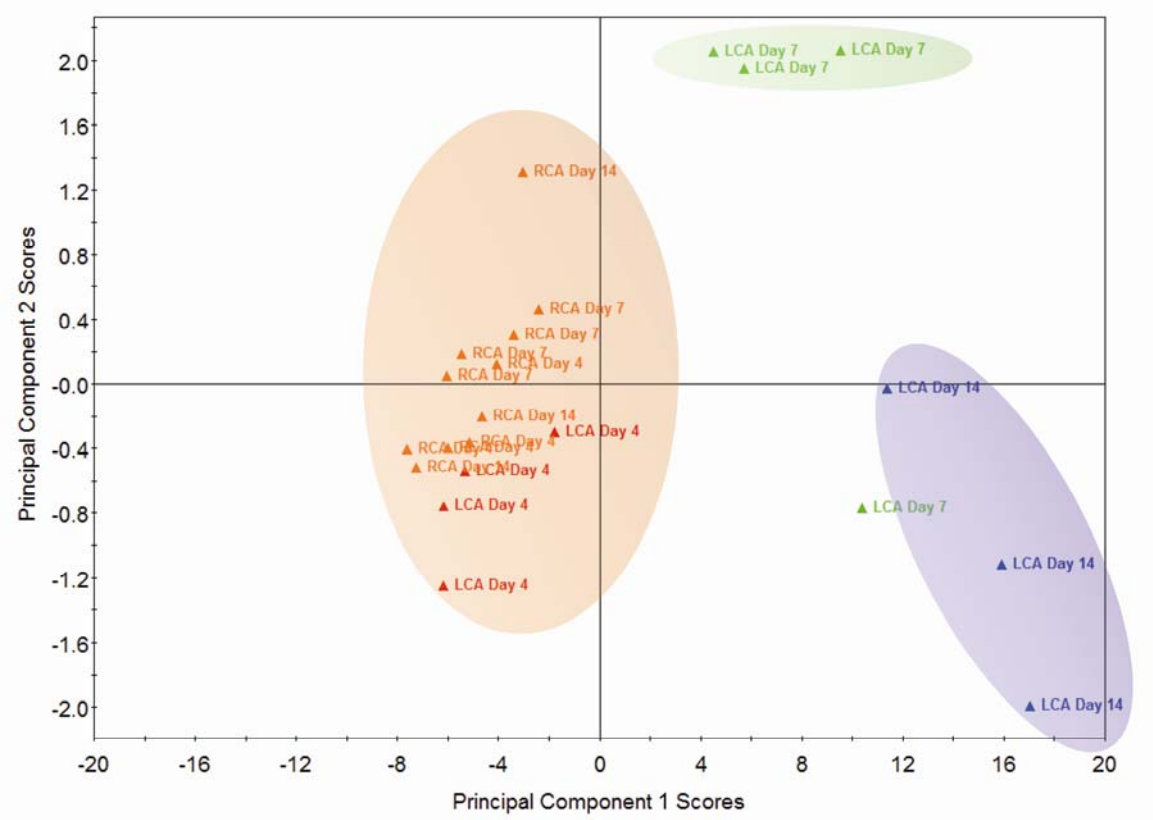

Supplemental Figure VI. PLSR modeling distinguishes time sensitive changes in cytokine and chemokine gene expression following partial carotid ligation. The scores plot of the contributions of individual LCA and RCA samples to the trained model separates time and flow conditions that induce expression of inflammatory cytokines from those that do not. Plot shows relatively uninflamed samples, LCA samples at 4 days post-ligation (red symbols) and RCA samples at any time point (orange symbols), versus samples showing a progressive increase in inflammation; LCA at 7 days post-ligation (green symbols) and LCA at 14 days post-ligation (blue symbols). Samples grouped by similar gene expression profiles are depicted by colored ovals.

Supplemental Figure VII.

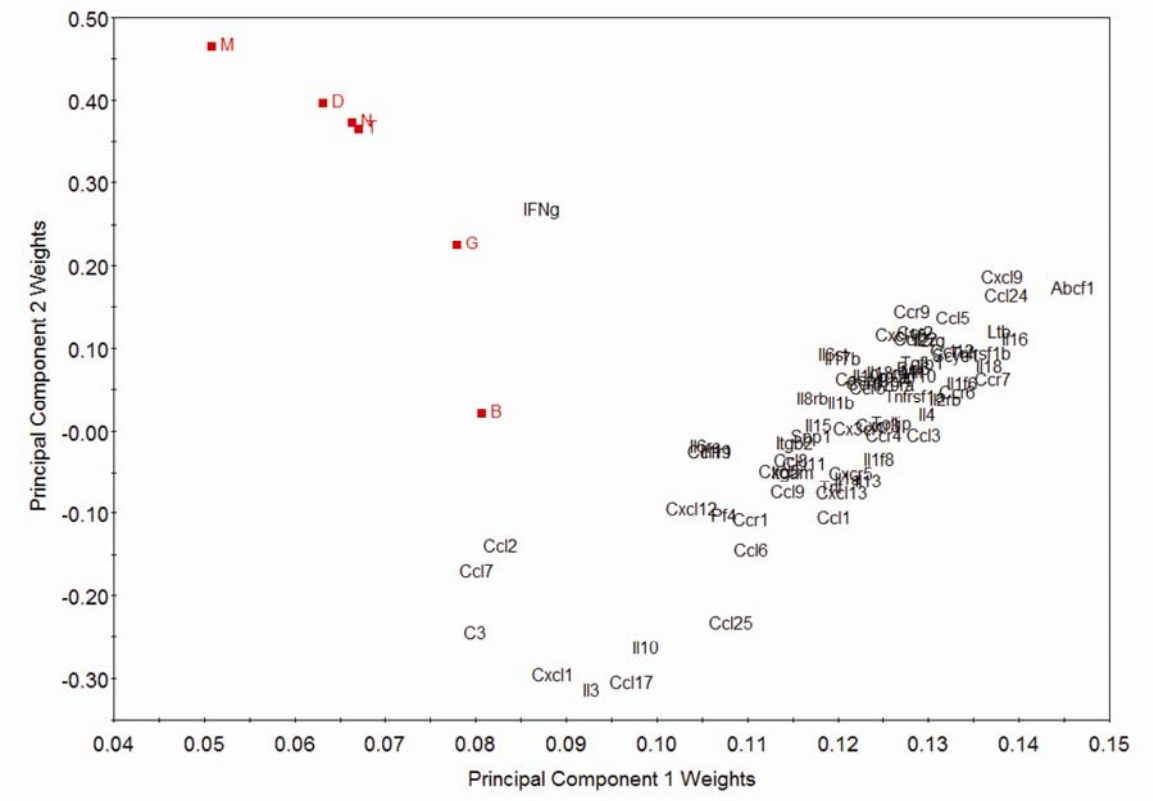

Supplemental Figure VII. PLSR modeling links IFNγ expression with increased leukocyte accumulation in flow-disturbed arterial wall at 7 days, preceding increased inflammation and plaque growth at 14 days post-ligation. The loading scatterplot of weights projects arterial wall leukocyte numbers from the flow cytometry experiments (red squares) on the same plot as changes in cytokine and chemokine expression from the qPCR array data set (black). Data from our PCR primer set for IFNγ has been substituted for the original array data. B, B-cells; T, T-cells, D, DCs, N, NK cells, M, monocyte/macrophages; G, granulocytes.

References

1. Nam D, Ni CW, Rezvan A, Suo J, Budzyn K, Llanos A, Harrison DG, Giddens DP, Jo H. A model of disturbed flow-induced atherosclerosis in mouse carotid artery by partial ligation and a simple method of RNA isolation from carotid endothelium. *J Vis Exp*. 2010
2. Nam D, Ni CW, Rezvan A, Suo J, Budzyn K, Llanos A, Harrison D, Giddens D, Jo H. Partial carotid ligation is a model of acutely induced disturbed flow, leading to rapid endothelial dysfunction and atherosclerosis. *Am J Physiol Heart Circ Physiol*. 2009;297:H1535-1543
3. Paigen B, Morrow A, Holmes PA, Mitchell D, Williams RA. Quantitative assessment of atherosclerotic lesions in mice. *Atherosclerosis*. 1987;68:231-240
4. Galkina E, Kadl A, Sanders J, Varughese D, Sarembock IJ, Ley K. Lymphocyte recruitment into the aortic wall before and during development of atherosclerosis is partially L-selectin dependent. *J Exp Med*. 2006;203:1273-1282
5. Perfetto SP, Ambrozak D, Nguyen R, Chattopadhyay P, Roederer M. Quality assurance for polychromatic flow cytometry. *Nat Protoc*. 2006;1:1522-1530
6. Roederer M. Multiparameter facs analysis. *Curr Protoc Immunol*. 2002;Chapter 5:Unit 5 8
7. Roederer M. Compensation in flow cytometry. *Curr Protoc Cytom*. 2002;Chapter 1:Unit 1 14
8. Li L, Chen W, Rezvan A, Jo H, Harrison DG. Tetrahydrobiopterin deficiency and nitric oxide synthase uncoupling contribute to atherosclerosis induced by disturbed flow. *Arterioscler Thromb Vasc Biol*. 2011
9. Kemp ML, Wille L, Lewis CL, Nicholson LB, Lauffenburger DA. Quantitative network signal combinations downstream of TCR activation can predict IL-2 production response. *J Immunol*. 2007;178:4984-4992

10. Miller-Jensen K, Janes KA, Brugge JS, Lauffenburger DA. Common effector processing mediates cell-specific responses to stimuli. *Nature*. 2007;448:604-608

11. Gaudet S, Janes KA, Albeck JG, Pace EA, Lauffenburger DA, Sorger PK. A compendium of signals and responses triggered by prodeath and prosurvival cytokines. *Mol Cell Proteomics*. 2005;4:1569-1590

12. Janes KA, Albeck JG, Gaudet S, Sorger PK, Lauffenburger DA, Yaffe MB. A systems model of signaling identifies a molecular basis set for cytokine-induced apoptosis. *Science*. 2005;310:1646-1653

13. Janes KA, Kelly JR, Gaudet S, Albeck JG, Sorger PK, Lauffenburger DA. Cue-signal-response analysis of TNF-induced apoptosis by partial least squares regression of dynamic multivariate data. *J Comput Biol*. 2004;11:544-561

14. Rivet CA, Hill AS, Lu H, Kemp ML. Predicting cytotoxic T-cell age from multivariate analysis of static and dynamic biomarkers. *Mol Cell Proteomics*. 2011;10:M110 003921